Video Article

Simultaneous Electroencephalography, Real-time Measurement of Lactate Concentration and Optogenetic Manipulation of Neuronal Activity in the Rodent Cerebral Cortex

William C. Clegern[1], Michele E. Moore[1], Michelle A. Schmidt[1], Jonathan Wisor[1]

[1]Department of Veterinary & Comparative Anatomy, Pharmacology and Physiology, Sleep and Performance Research Center, WWAMI Medical Education Program, Washington State University

Correspondence to: Jonathan Wisor at J_Wisor@wsu.edu

URL: https://www.jove.com/video/4328
DOI: doi:10.3791/4328

Keywords: Neuroscience, Issue 70, Physiology, Anatomy, Medicine, Pharmacology, Surgery, Sleep, rapid eye movement, glucose, glycolysis, pyramidal neurons, channelrhodopsin, optogenetics, optogenetic stimulation, electroencephalogram, EEG, EMG, brain, animal model

Date Published: 12/19/2012

Citation: Clegern, W.C., Moore, M.E., Schmidt, M.A., Wisor, J. Simultaneous Electroencephalography, Real-time Measurement of Lactate Concentration and Optogenetic Manipulation of Neuronal Activity in the Rodent Cerebral Cortex. *J. Vis. Exp.* (70), e4328, doi:10.3791/4328 (2012).

Abstract

Although the brain represents less than 5% of the body by mass, it utilizes approximately one quarter of the glucose used by the body at rest[1]. The function of non rapid eye movement sleep (NREMS), the largest portion of sleep by time, is uncertain. However, one salient feature of NREMS is a significant reduction in the rate of cerebral glucose utilization relative to wakefulness[2-4]. This and other findings have led to the widely held belief that sleep serves a function related to cerebral metabolism. Yet, the mechanisms underlying the reduction in cerebral glucose metabolism during NREMS remain to be elucidated.

One phenomenon associated with NREMS that might impact cerebral metabolic rate is the occurrence of slow waves, oscillations at frequencies less than 4 Hz, in the electroencephalogram[5,6]. These slow waves detected at the level of the skull or cerebral cortical surface reflect the oscillations of underlying neurons between a depolarized/up state and a hyperpolarized/down state[7]. During the down state, cells do not undergo action potentials for intervals of up to several hundred milliseconds. Restoration of ionic concentration gradients subsequent to action potentials represents a significant metabolic load on the cell[8]; absence of action potentials during down states associated with NREMS may contribute to reduced metabolism relative to wake.

Two technical challenges had to be addressed in order for this hypothetical relationship to be tested. First, it was necessary to measure cerebral glycolytic metabolism with a temporal resolution reflective of the dynamics of the cerebral EEG (that is, over seconds rather than minutes). To do so, we measured the concentration of lactate, the product of aerobic glycolysis, and therefore a readout of the rate of glucose metabolism in the brains of mice. Lactate was measured using a lactate oxidase based real time sensor embedded in the frontal cortex. The sensing mechanism consists of a platinum-iridium electrode surrounded by a layer of lactate oxidase molecules. Metabolism of lactate by lactate oxidase produces hydrogen peroxide, which produces a current in the platinum-iridium electrode. So a ramping up of cerebral glycolysis provides an increase in the concentration of substrate for lactate oxidase, which then is reflected in increased current at the sensing electrode. It was additionally necessary to measure these variables while manipulating the excitability of the cerebral cortex, in order to isolate this variable from other facets of NREMS.

We devised an experimental system for simultaneous measurement of neuronal activity via the elecetroencephalogram, measurement of glycolytic flux via a lactate biosensor, and manipulation of cerebral cortical neuronal activity via optogenetic activation of pyramidal neurons. We have utilized this system to document the relationship between sleep-related electroencephalographic waveforms and the moment-to-moment dynamics of lactate concentration in the cerebral cortex. The protocol may be useful for any individual interested in studying, in freely behaving rodents, the relationship between neuronal activity measured at the electroencephalographic level and cellular energetics within the brain.

Video Link

The video component of this article can be found at https://www.jove.com/video/4328/

Protocol

1. Surgical Preparation of Animals

1. Experimental Subjects

Use mice of the B6.Cg-Tg(Thy1-COP4/eYFP)18Gfng/J transgenic line[9]; JAX strain #7612) or other mice expressing the blue light-sensitive cation channel, Channelrhodopsin-2, in cerebral cortical neurons. Application of blue light to the cerebral cortex of the B6.Cg-Tg(Thy1-COP4/eYFP)18Gfng/J transgenic line causes the pyramidal neurons expressing Channelrhodopsin-2 to depolarize and undergo action potentials[9,10].

As a consequence of pyramidal cell activation, local interneurons are activated, and the change in potential is propagated to neurons beyond the site of stimulation[10]. Perform surgery under sterile conditions in adherence to applicable regulatory guidelines: autoclave surgical tools and softpacks (surgical field, gauze pads); hot bead sterilize all heat-tolerant implanted metal devices (cannulas, screws and wires) for 30-sec; Disinfect heat-intolerant implantable devices (fiber optic cable, plastic connector) with a 10-sec dip in ethanol; blow ethanol-dipped items dry by application of canned air.

2. Anesthesia, Stereotaxic Placement and Clearance of Skull

Use the IMPAC[6] Integrated Multi Patient (Vet Equip Inc) system to anesthetize the mouse. Use 5% Isoflurane/95% Oxygen for induction and 3% Isoflurane/97% oxygen for maintenance during surgery. Place the animal on a circulating-water blanket set to 37 C. It is not necessary to monitor body temperature if the blanket is kept at this temperature.

3. Preparing the Skull for Implantation

Prepare the incision site by shaving all fur from the top of the skull. The shaved area should extend laterally from ear to ear and anterior-posterior from the eyes to the posterior end of the skull. Disinfect the exposed skin with three consecutive swabs of betadine followed by ethanol. Make a medial incision on the top of the skull, from between the eyes to the back of the skull. Clean the skull with hydrogen peroxide and sterile saline (0.9% NaCl). Control bleeding with a cauterizing tool. Locate and mark bregma and lambda for determining stereotaxic coordinates. Stereotaxic coordinates for electrode/optogenetic stimulus configurations that we have used are presented in **Table 1** and shown schematically in **Figure 1A**.

4. Preparation of the Implantation Sites on Skull

Use a high speed dental drill with a 0.5 mm ball burr bit to establish each implantation site in the skull. Chamfer the external margin of each hole using a 0.7 mm ball burr bit to facilitate screw insertion.

5. Insertion and Securing of Cannulas, EMG Leads and EEG Leads

Insert EEG screws (0.8 mm in length, with 2 cm of uncoated 30-gauge tinned-copper bus wire pre-soldered to screw head) into the holes and drive them in with a slotted hand screwdriver approximately 4-5 revolutions to obtain the desired depth. Hold guide cannulas in place with a stereotaxic cannula holder and then affix them to the skull and anchors with acrylic cement. Each guide cannula should contain a dummy cannula/stylet (Plastics One, part # C312 DC\1) from the time of surgery to the time of experimentation (10-14 days) to maintain patency.

6. Closing Surgical Site

Once EEGs and guide cannulas are positioned in the skull, bond them together with dental acrylic cement (Lang Dental - Ortho-Jet cement). After cement sets, position the plastic connector (Pinnacle Technology part # 8402) above the dried cement mound. Solder the ends of the wires emanating from EEG leads to the contacts on the plastic connector. Encase the wire leads in cement. Then draw the EMG wires through the nuchal muscles by sliding them into the barrel of a 21ga needle pierced through muscle. Tie a double surgeon's knot of 5-0 nylon suture around these wires just distal to where they exit the muscle. Suture back together the skin that was retracted to access the muscle tissue with single interrupted surgeon knots, using a reverse cutting P-3 needle and 5-0 nylon suture.

7. Post-operative Analgesia and Recovery

Administer buprenorphine as an analgesic (0.1 mg/kg, subcutaneous) and flunixin meglumine (0.1 mg/kg, subcutaneous) as an anti-inflammatory immediately after surgery, and daily on days 1-2 post-surgery. Allow animals to recover in standard colony housing conditions for at least seven days before experimentation. With no additional care beyond standard colony housing, cannulas can be expected to remain patent for at least two weeks with the indwelling stylets secured in place. EEG and EMG sensors can also be expected to retain functionality for this duration.

2. Generation of Timed Light Pulses

1. Programming of MC Stimulus Unit

Connect the MC-Stimulus unit (Multi-Channel Systems) via a USB connection to a desktop computer. Use the spreadsheet-like MC-Stimulus user interface to program the MC Stimulus unit. Enter the desired TTL (transistor-transistor logic) voltage for the on period, the durations of stimulus on and off periods, the number of cycles per second desired, and the total number of repeated cycles for the entire stimulus session. For further details see MC-Stimulus technical manual:

http://www.multichannelsystems.com/sites/multichannelsystems.com/files/documents/manuals/STG4002_Manual.pdf

3. Manufacture/Assembly of Fiber Optic Probes for Light Delivery to the Cerebral Cortex

1. Supplies and equipment needed are found at: http://www.thorlabs.com/Thorcat/1100/1166-D02.pdf
2. Cutting and polishing of fiber optic cables. http://www.thorlabs.com/Thorcat/1100/1166-D02.pdf

4. Assembly of Rodent Optogenetic Stimulation System

1. Interface of MC-Stimulus Unit and Laser

Once the MC-Stimulus unit is programmed, run it as a stand-alone signal generator of a 5-Volt binary ON/OFF signal. Connect the MC-Stimulus unit to the TTL enabled power unit of the laser with BNC connectors.

2. Producing Laser Output via Fiber Optic Cable

Use the digital display and variable power output dial of the laser power unit to manually adjust the power output of the laser. Connect the laser power unit to the laser via a ribbon cable. Connect the female FC (ferrule connector) fiber adapter of the laser to the male FC connector on the fiber optic patch cable (a 3 m length, 200 µm diameter glass conduction fiber encased in light reflecting acrylate polymer cladding).

3. Conveying the Laser to the Animal: Rotary Commutator

Connect the originating fiber optic cable (3 m in length) and the delivery fiber optic cable (45 cm in length) to opposing ends of the optic rotary joint encasing two collimating lenses (Doric lenses). The fiber optic rotary joint serves as a commutator: as the animal moves about its cage, the rotary joint rotates to prevent breakage of the fiber optic cables. Use plastic cable ties to affix the commutator to a metal stand placed above the cylindrical cage in which the animal is housed.

4. Attaching Delivery Fiber Optic Cable to Head

Restrain the mouse by using one hand to pin the mouse under a cupped palm. Orient the head between the experimenter's middle and index finger. Remove the dummy cannula from the guide cannula placed for the fiber optic cannula. Clear the guide cannula of debris using a sterile 25ga needle. Insert the fiber optic cable by hand and fasten it to the fiber optic guide cannula with a threaded screw cap salvaged from a dummy cannula. Control the depth of insertion of the fiber optic cable in the brain by a suture knot tied on the fiber optic cable at a fixed distance from the flat-cleaved end. The entire experimental apparatus is shown in **Figure 1B**.

5. Measurement of EEG-defined Sleep and Lactate Concentration during Optogenetic Stimulation

1. Precalibration of the Lactate Sensor

Pre-calibration of the lactate sensor is performed with an *in vitro* kit (Pinnacle Technology part # 7000-K1-T). The sensor is equilibrated in phosphate buffered saline (pH 7.4), then exposed to three concentrations of L-lactate in stepwise fashion per manufacturer protocols.

2. Insertion of the Lactate Sensor and EEG Cable

Insert the pre-calibrated sensor into the skull-mounted lactate guide cannula in a manner identical to the fiber optic cable insertion procedure (section 4.4). Connect the lactate sensor to the preamplifier of the Pinnacle 8,400 biosensor with bipolar plug connectors. Attach this preamplifier to the 8-pin connector on the surgically-implanted headmount.

3. Establishing Optogenetic Stimulus Intensity

Before collecting data, use the laser intensity control knob to adjust the intensity of the optogenetic stimulus. The amplitude of the EEG response will vary across animals, due to factors that have not been studied systematically, and must be verified by visual inspection at the onset of stimulation. In practice, an intensity of 80-120 µWatts will typically produce an increase in EEG amplitude of approximately 50% at the frequency of stimulation. Post-hoc fast Fourier transform analysis (see section 5.5) is necessary to quantify the absolute magnitude of the response.

4. Data Collection

Collect data using the Pinnacle 8400 system: http://pinnaclet.com/pal-8400.html.

5. Data Processing with Neuroscore

Classify sleep states by visual inspection of the EEG and EMG data with the Neuroscore interface (DataSciences, International: http://www.datasci.com/products/software/NeuroScore_CNS_Software.asp) or the Sirenia interface (Pinnacle Technology: http://www.pinnaclet.com/sirenia.html). Process data in ten-second epochs as wake, non-rapid eye movement sleep, or rapid eye movement sleep based on EEG and EMG. Save data as Microsoft Excel spreadsheets for additional analysis and statistical testing.

Representative Results

As shown in **Figure 2**, a mouse equipped for optogenetic stimulation and lactate/EEG/EMG data collection underwent spontaneous sleep/wake state transitions while EEG, EMG and cerebral lactate concentration were monitored continuously. Current at the lactate sensor increased during periods of low amplitude EEG and decreased during periods of high amplitude EEG. As shown in **Figure 3**, both channels of the EEG are responsive to optogenetic stimuli delivered in the frontal cortex.

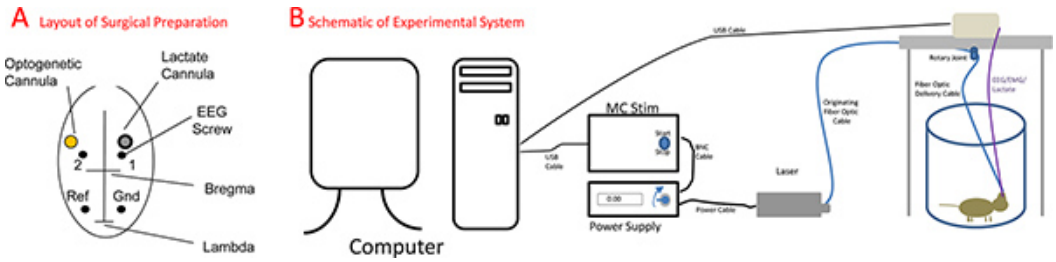

Figure 1. A) Schematic representation of the surgically-implanted EEG electrodes, lactate sensor and cannula for optogenetic stimulation. B) Schematic representation of the entire experimental system. 1, EEG lead 1. 2, EEG lead 2. Gnd, EEG ground screw. Ref, EEG reference screw. Click here to view larger figure.

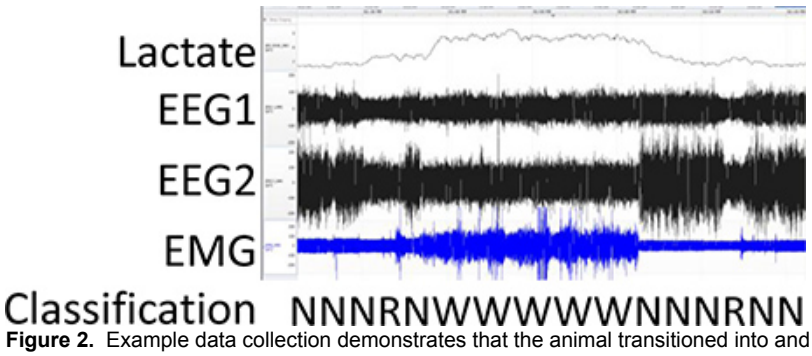

Figure 2. Example data collection demonstrates that the animal transitioned into and out of sleep while instrumented for recordings using the biosensor/optogenetic stimulus configuration seen in **Figure 1A**. Optogenetic stimulation was not applied during the interval shown here. Wake (W) and the two subtypes of sleep, rapid eye movement sleep (R) and non-rapid eye movement sleep (N) are defined based on the electroencephalogram (EEG) and the electromyogram (EMG). High amplitude EMG accompanied by low amplitude EEG defines wake. Low amplitude EMG accompanied by low amplitude EEG defines rapid eye movement sleep. Low amplitude EMG accompanied by high amplitude EEG defines non-rapid eye movement sleep. Lactate biosensor current rises as a function of low amplitude EEG (*i.e.*, during both wake and rapid eye movement sleep) and falls as a function of high amplitude EEG (*i.e.*, during non-rapid eye movement sleep).

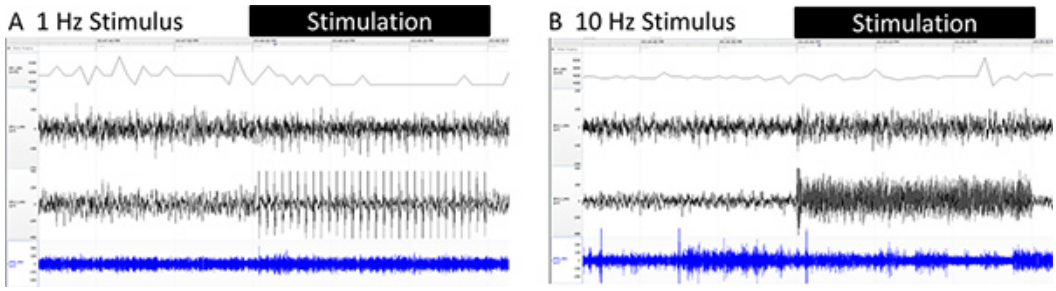

Figure 3. Representative data from animals subjected to optogenetic stimulation at 1 Hz (A) or 10 Hz (B) using the biosensor/optogenetic stimulus configuration seen in **Figure 1A**. Traces represent 60-sec recordings. The timing of a 30-sec interval of stimulation is indicated at the top of each panel. Click here to view larger figure.

Frontal Stimulation- Relative to Bregma (mm)			
	Ant/Post	**Lat**	**D/V**
EEG1	+2.2	+1.6	--
EEG2	+2.2	-1.6	--
Reference	-3.5	-1.5	--
Ground	-3.5	1.5	--
Lactate Cannula	+1.0	+1.6	-0.5
Optogenetic Cannula	+1.0	-1.6	-0.5

Table 1. Stereotaxic coordinates of surgically implanted devices.

Discussion

The methods presented here allow one to measure the relationship between sleep and changes in the brain concentration of the glycolytic intermediate lactate on a time scale not previously possible. Animals undergo spontaneous transitions between wake, NREMS and REMS.

Furthermore, we are able to apply optogenetic stimuli while animals undergo these transitions. Data collected to date demonstrate that both spontaneous and induced waves impact on the readout of a lactate oxidase-based biosensor.

One could construct experimental systems similar to the one described here with equipment and software from other sources. Alternative sources of polysomnographic systems suitable for rodents include Data Sciences International[11], and Embla[12]. Software for sleep state classification is available from Somnologica[12], Sleep Sign[13] and Icelus[14]. Amperometric biosensors for measurement of lactate are available from Quanteon[15]. To our knowledge, Pinnacle Technology offers the only system in which biosensors, EEG and EMG can be measured simultaneously with one software interface.

We have measured changes in both lactate concentration and the EEG distal to the site of optogenetic stimulation. Effects of optogenetic stimulation at such distal sites confirms that optogenetically-induced potential changes are propagated beyond the site of stimulation. One could measure these parameters directly within the area of cortex exposed to light, but measuring them elsewhere assures that responses are due to wave propagation, as opposed to an artifactual response of the biosensor to light exposure (as documented[16]). Optogenetically-induced 1-Hz waves are distinct from sleep slow waves in that they are not synchronized by subcortical projecting neurons. As such, they do not occur in stereotyped temporal relationships with other sleep-related phenomena, such as spindles and K-complexes[17]. Whether optogenetic stimulation mimics other effects of natural slow waves (such as changes in synaptic strength[18] or homoeostatic changes in EEG slow wave activity[11]) is uncertain. The methods described here could be used to address this question in future studies.

Animals are tethered by both the wires conveying biopotentials from animal to computer and the fiber optic cable that conveys blue light into the cerebral cortex. Both wireless EEG/bioanalyte recording systems (http://pinnaclet.com/biosensor-recording-sys/fixed-frequency.html) and wireless optogenetic stimulation devices[19] have been reported. However, the two have not been integrated into a single working system to our knowledge. Despite the restraint associated with a tethering cable, animals are frequently seen moving around their cages, and the amount of time spent asleep is typical of mice studied in similar experimental situations. Sensors compatible with this system are available for the measurement of other bioanalytes, including glucose and glutamate. The system is therefore likely to be useful in other experimental situations in which behavior, EEG and bioanalyte concentrations are analyzed.

Disclosures

No conflicts of interest declared.

Acknowledgements

Research funded by Department of Defense (Defense Advanced Research Projects Agency, Young Faculty Award, Grant Number N66001-09-1-2117) and NINDS (R15NS070734).

References

1. Magistretti, P. Brain Energy Metabolism. In: *Fundamental Neuroscience*., Zigmond, M.J., Bloom, F.E., Landis, S.C., Roberts, J.L., & Squire, L.R., eds., Academic Press, New York, 389-413 (1999).
2. Maquet P, *et al.* Cerebral glucose utilization during sleep-wake cycle in man determined by positron emission tomography and [18F]2-fluoro-2-deoxy-D-glucose method. *Brain Res.* **513**(1), 136-143 (1990).
3. Buchsbaum, M.S., *et al.* Regional cerebral glucose metabolic rate in human sleep assessed by positron emission tomography. *Life Sci.* **45** (15), 1349-1356 (1989).
4. Kennedy, C., *et al.* Local cerebral glucose utilization in non-rapid eye movement sleep. *Nature.* **297** (5864), 325-327 (1982).
5. Pappenheimer, J.R., Koski, G., Fencl, V., Karnovsky, M.L., & Krueger, J. Extraction of sleep-promoting factor S from cerebrospinal fluid and from brains of sleep-deprived animals. *J. Neurophysiol.* **38** (6), 1299-1311 (1975).
6. Borbely, A.A. & Achermann, P. Sleep homeostasis and models of sleep regulation. In: *Principles and Practice of Sleep Medicine*., Kryger, M.H., Roth, T., & Dement, W.C., eds., W.B. Saunders, Philadelphia, 3rd Edition, 377-390 (2004).
7. Destexhe, A., Contreras, D., & Steriade, M. Spatiotemporal analysis of local field potentials and unit discharges in cat cerebral cortex during natural wake and sleep states. *J. Neurosci.* **19** (11), 4595-4608 (1999).
8. Astrup, J., Sorensen, P.M., & Sorensen, H.R. Oxygen and glucose consumption related to Na^+-K^+ transport in canine brain. *Stroke.* **12** (6), 726-730 (1981).
9. Arenkiel, B.R., *et al. In vivo* light-induced activation of neural circuitry in transgenic mice expressing channelrhodopsin-2. *Neuron.* **54** (2), 205-218 (2007).
10. Mateo, C., *et al. In Vivo* Optogenetic Stimulation of Neocortical Excitatory Neurons Drives Brain-State-Dependent Inhibition. *Curr. Biol.*, (2011).
11. Wisor, J.P. & Clegern, W.C. Quantification of short-term slow wave sleep homeostasis and its disruption by minocycline in the laboratory mouse. *Neurosci. Lett.* **490** (3), 165-169 (2011).
12. El Yacoubi, M., *et al.* Behavioral, neurochemical, and electrophysiological characterization of a genetic mouse model of depression. *Proc. Natl. Acad. Sci. U.S.A.* **100** (10), 6227-6232 (2003).
13. Tsunematsu, T., *et al.* Acute optogenetic silencing of orexin/hypocretin neurons induces slow-wave sleep in mice. *J. Neurosci.* **31** (29), 10529-10539 (2011).
14. Le, S., Gruner, J.A., Mathiasen, J.R., Marino, M.J., & Schaffhauser, H. Correlation between *ex vivo* receptor occupancy and wake-promoting activity of selective H3 receptor antagonists. *J. Pharmacol. Exp. Ther.* **325** (3), 902-909 (2008).
15. Burmeister, J.J., Palmer, M., & Gerhardt, G.A. L-lactate measures in brain tissue with ceramic-based multisite microelectrodes. *Biosens. Bioelectron.* **20**(9), 1772-1779 (2005).

16. Cardin, J.A., *et al.* Targeted optogenetic stimulation and recording of neurons *in vivo* using cell-type-specific expression of Channelrhodopsin-2. *Nat. Protoc.* **5**(2), 247-254 (2010).
17. Destexhe, A., Contreras, D., & Steriade, M. Cortically-induced coherence of a thalamic-generated oscillation. *Neuroscience.* **92** (2), 427-443 (1999).
18. Liu, Z.W., Faraguna, U., Cirelli, C., Tononi, G., & Gao. X.B. Direct evidence for wake-related increases and sleep-related decreases in synaptic strength in rodent cortex. *J. Neurosci.* **30** (25), 8671-8675 (2010).
19. Iwai, Y., Honda, S., Ozeki, H., Hashimoto, M., & Hirase, H. A simple head-mountable LED device for chronic stimulation of optogenetic molecules in freely moving mice. *Neurosci. Res.* **70** (1), 124-127 (2011).

